Journal of Applied Physics

Effect of β-stabilizer elements on stacking faults energies and ductility of α-titanium using first-principles calculations

Cite as: J. Appl. Phys. **120**, 175105 (2016); https://doi.org/10.1063/1.4966939
Submitted: 25 August 2016 . Accepted: 20 October 2016 . Published Online: 04 November 2016

R. Salloom, R. Banerjee, and S. G. Srinivasan

Effect of β-stabilizer elements on stacking faults energies and ductility of α-titanium using first-principles calculations

R. Salloom, R. Banerjee, and S. G. Srinivasan[a)]
Department of Materials Science and Engineering, University of North Texas, Denton, Texas 76205, USA

(Received 25 August 2016; accepted 20 October 2016; published online 4 November 2016)

The effect of W, Mo, V, Ta, and Nb, five common β-stabilizing substitutional elements, on α-Ti stacking fault energy has been studied using first principle calculations. The generalized stacking fault energy (GSFE) curves have been determined for different concentrations of β-stabilizers at the fault plane using supercells with up to 360 atoms. Both basal and prismatic slip systems with the stable (γ_{SF}) and unstable (γ_{USF}) stacking faults and twinning fault energies were determined. All the alloying elements reduce the stacking fault energy for Ti for both basal and prismatic slip. At higher concentration of 25 at. % of V, Ta, and Nb at the slip plane, the basal slip becomes more favorable than the prismatic slip in Ti. Ti-Mo and Ti-W systems also show a significant shift in the GSFE curve towards a higher shear deformation strain along $\langle 01\bar{1}0\rangle$ due to the change in bond character between Ti and those two elements. Using Rice criterion, which employs γ_S/γ_{USF} ratio to estimate ductility, we show that all the alloying elements likely improve the ductility of α-Ti with Ti-25 at. % Nb exhibiting the most ductile behavior. However, according to the Tadmor and Bernstein model, all the alloying elements considered here do not improve the partial dislocation emission or the twinning propensity in spite of decreasing the stacking fault energies for α-Ti and. Hence, a better empirical model that incorporates changes in the character of directional bonding upon alloying is needed to estimate how alloying influences ductility in hcp metals. *Published by AIP Publishing*. [http://dx.doi.org/10.1063/1.4966939]

I. INTRODUCTION

Ti and its alloys are well suited for structural application in automotive and aerospace industries because of their high strength-to-weight ratio and good corrosion resistance in many environments. In addition, they are attractive choices for bio-medical applications due to high compatibility with the human body tissue.[1] However, the presence of fewer than five independent slip systems in hexagonal closed-packed (hcp) Ti leads to its limited formability at room temperature.[2]

Numerous Ti alloy compositions, with different combinations of microstructures and properties, have been developed often by slow, trial and error methods. Computational approaches such as first principle calculations can provide the theoretical basis to guide the development of advanced Ti alloys and also perhaps identify composition of existing alloys with better properties. A computational assessment of mechanical behavior is an indispensable initial step, and it includes the study of dislocations and the associated stacking faults and twin fault energies. The Generalized Stacking Fault Energy (GSFE) surface quantifies energy per unit area required to shear a crystal on a potential slip plane parallel to the displacement vector. This energy provides a significant insight on the mechanical properties by elucidating the mobility and core structure of dislocations.[3] The stacking fault energy of a material can often be tailored via alloying. In fact, the values of this energy dictate the separation width during dissociation of a lattice dislocation into partials and control the climb and cross slip movements of dislocation.[4] The low values of the stacking fault energy increase the splitting distance between partial dislocations, and this enhances the tendency for twinning, decreases the steady state creep by suppressing the climb and cross-slip movements,[5,6] and improves strength and ductility by increasing the work hardening rate.[1,7] Therefore, it is important to understand the effects of alloying elements on the stacking fault energy in a technologically important metal such as α-Ti.

The experimental study of stacking faults of Ti is difficult due to the dense nature of dislocation core and small separation distance between partials. Therefore, the atomistic simulation of GSFE of Ti is an effective and accurate method to investigate the stacking fault and the core structure of dislocations.[8] Ti deforms predominantly by $\{10\bar{1}0\}$ prismatic slip rather than {0001} basal slip due to low separation distance between the basal planes and the directional bonding of the d-electron.[2] Adding alloying elements is hypothesized to change the prismatic slip preference of Ti by changing the bonding behavior at the slip plane. For example, adding Al was found to cause a transition from the prismatic slip to the basal slip in Ti.[6] The effects of some alloying elements, such as Al, and interstitial C, H, N, and O on the basal stacking fault energy of Ti have been reported previously.[6,9] Also, the increased prismatic stacking fault energy of Ti with interstitial O addition has also been reported in the previous studies.[10,11] However, the effect of important β-stabilizer elements on basal and prismatic stacking fault energies is yet to be investigated.

[a)]Author to whom correspondence should be addressed. Electronic mail: Srinivasan.Srivilliputhur@unt.edu.

A perfect ***a*** dislocation of the basal plane $1/3\langle 11\bar{2}0\rangle$ in hcp metals energetically favors the dissociation into Shockley partials according to the reaction

$$\frac{1}{3}\langle 11\bar{2}0\rangle \rightarrow \frac{1}{3}\langle 10\bar{1}0\rangle + \frac{1}{3}\langle 01\bar{1}0\rangle.$$

Therefore, a partial dislocation deformation is preferred for the basal plane. However, some hcp metals such as Ti, Zr, and Hf with non-ideal c/a ratio have a dominant prismatic slip system $\{10\bar{1}0\}\langle 11\bar{2}0\rangle$.[2] Also, Vitek and Igarashi[12] proposed that the core of screw dislocation with $1/3\langle 11\bar{2}0\rangle$ Burgers vector can dissociate on the prismatic plane into partials and show a metastable stacking fault by the reaction

$$\frac{1}{3}\langle 11\bar{2}0\rangle \rightarrow \frac{1}{6}\langle 11\bar{2}x\rangle + \frac{1}{6}\langle 11\bar{2}\bar{x}\rangle,$$

where x varies from 0 to 1.2 and depends on the material. As a high stacking fault energy metal, Ti has limited formability due to the lack of multiple slip systems, so activating slip systems other than the primary prismatic slip would have a substantial effect on Ti strength and ductility. The changing of perfect hcp stacking sequence from ABABABAB to ABABCACA through the basal slip of 1/3 along $\langle 10\bar{1}0\rangle$ leads to the formation of intrinsic deformation stacking fault I2 which affects the deformation behavior of the hcp metals due to its influence on the dislocation dissociation. Therefore, studying these faults will predict the possible deformation mechanism for α-Ti alloys at the atomic level.

Understanding the mechanism and estimating the energy barrier for dislocation dissociation is an important input to develop modern tailored Ti alloys, which possess both good ductility and strength. The density functional theory (DFT) based calculations will enable us to investigate the effect of several β-stabilizer elements on the Ti plastic behavior at the atomic level. In this work, we will investigate the influence of W, Mo, V, Ta, and Nb on the energy barrier for dislocation dissociation and twin nucleation by studying the basal I2, twin T2, and prismatic stacking fault energies of Ti with different concentrations of solute atoms. In addition, studying the effects of selected alloying elements on bond morphology of Ti at the stacking fault plane will also provide qualitative insight into the role of electron charge accumulation and depletion on the bond strength of Ti. The first-principle calculations and computational methodology are covered in Section II. The calculated stacking fault energies for Ti and Ti-X systems are discussed in addition to the bond morphology investigation in Section III. Finally, a summary is presented in Section IV.

II. COMPUTATIONAL METHODOLOGY

We use the well-known Vienna *Ab initio* Simulation Package (VASP) to study GSFE curves for basal I2 and prismatic slips of Ti.[13,14] A projector augmented wave (PAW) method is used to describe the core and valence electrons on s and d orbitals.[15] The exchange-correlation functional of Perdew–Burke–Ernzerhof is used for the Generalized Gradient Approximation (GGA-PBE).[16] A plane wave cut-off energy of 400 eV is used. The total energy convergence accuracy of 10^{-5} eV was chosen for electronic relaxation, and Methfessel-Paxton smearing of electronic occupancy was 0.2 eV. The k-point mesh for K points sampling is $15 \times 15 \times 9$ for Ti unit cell. These parameters yield a well-converged energy.

GSFE curves for the basal slip were calculated using an orthogonal supercell with 48 atoms and 12 atomic (0001) layers. 10 Å vacuum gap and relaxation of atoms normal to the slip plane were used. In order to generate a deformation stacking fault I2 for $(0001)/[\bar{1}100]$ slip system, top half of supercell perpendicular to (0001) was displaced by a/3 along the slip direction to form ABAB(C)ACAC sequence, and after that, a deformation twin(T2) was generated by displacing atomic planes 8–12 along the same direction to form ABAB(C)BABA atomic arrangements. For the prismatic stacking fault, another orthogonal supercell with 96 atoms and 24 atomic layers with 10 Å vacuum gap was used. The atomic layers 13–24 were displaced along $[1\bar{2}10]$ slip direction to generate a prismatic stacking fault. For the Ti-X alloys, we replaced one Ti atom on the stacking fault plane with an alloying element atom such as W, Mo, V, Ta, or Nb to study their effect on basal and prismatic stacking fault energies. The 48 and 96 atoms supercells are shown in Fig. 1. For broader understanding of the effect of these alloying elements on the stacking fault energy in Ti, different concentrations of alloying element at the slip plane will be used for each basal and prismatic slip systems. Two other supercells of 80 and 160 atoms for basal and prismatic slip systems, respectively, were used to quantify this effect. The purpose of choosing a lower concentration of solute atoms at the slip plane is to reduce the interaction between the alloying elements through decreasing the number of X-Ti-X bonds and that increases the distance between the alloying elements atoms at the slip plane. The atomic concentrations of the solute atoms on the slip plane for both basal and prismatic supercells are 25 at. % and 12.5 at. %. The total concentrations of the basal supercells were 2.08 at. % and 1.25 at. % for 25 at. % and 12.5 at. % fault plane concentrations, respectively, while the total concentrations for prismatic supercells were about 1 at. % and 0.6 at. % for 25 at. % and 12.5 at. % fault plane concentrations, respectively. It should be noted that the fault plane concentration of alloying elements is more appropriate than the overall concentration. The stacking fault energy is calculated as

$$\gamma = \frac{E_{sf} - E_{\mathrm{o}}}{\mathrm{A}},$$

where E_{sf} is the energy of the supercell with the stacking fault, E_{o} is the energy of the unfaulted supercell, and A is the area of the stacking fault.

Previous studies of the phase stabilities of binary Ti-X (X = W, Mo, V, Ta, and Nb)[17,18] systems showed that they have a stable α-phase at low concentrations of X, while the metastable β-phase becomes energetically more favorable than the α-phase when the concentration of X element becomes large enough, which is system dependent. In this

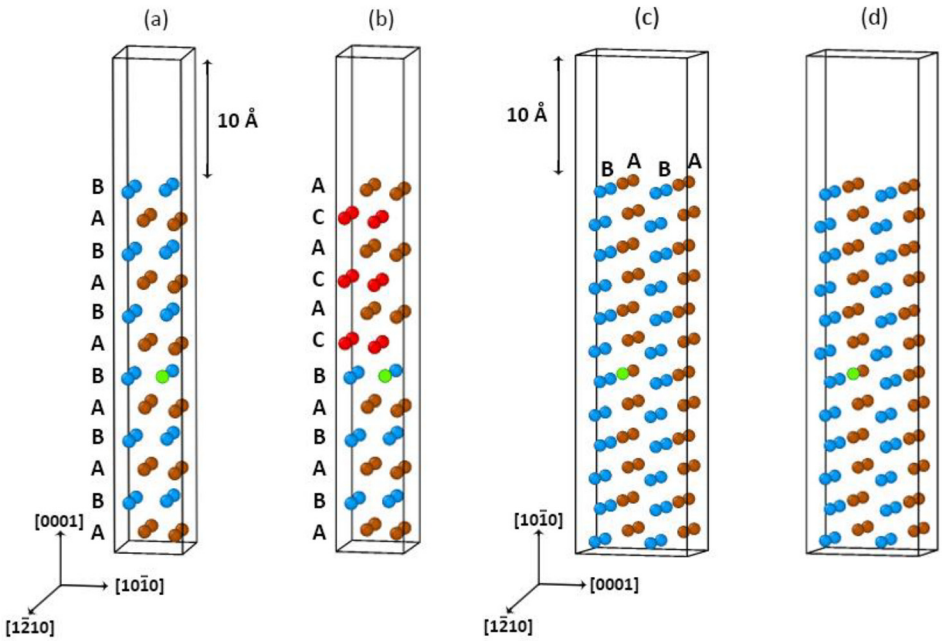

FIG. 1. (a) 48 atom supercell for basal slip before stacking fault creation. (b) 48 atoms supercell after a/3 displacement along $\langle 01\bar{1}0\rangle$. (c) 96 atoms supercell for prismatic slip before stacking fault creation. (d) 96 atoms supercell after 1/2 displacement along $\langle 1\bar{2}10\rangle$. The solute atoms are in green color. The brown, blue, and red atoms are for different atomic planes stacking.

study, we used low enough global concentrations of β-stabilizers to study single α-phase stable structures.

III. THE EFFECT OF ALLOYING ELEMENTS ON STACKING FAULTS AND TWINNING

The dislocation core structure in α-Ti can be understood by generalized stacking fault energy surface or gamma surface.[8] The γ-surface can be calculated by displacing a slip plane of interest by linear steps along possible slip directions and allows relaxation of atoms only normal to this slip plane. Fig. 2 presents the calculated γ-surfaces for basal and prismatic slips. Fig. 2(a) shows that the unstable stacking fault (γ_{USF}) for I2 for $\langle 01\bar{1}0\rangle$ in pure α-Ti is lower than that of $\langle 1\bar{2}10\rangle$, which makes the $\langle 01\bar{1}0\rangle$ the preferred energy path for the basal slip. On the other hand, the prismatic γ-surface [Fig. 2(b)] shows a preferred energy path, a long $\langle 1\bar{2}10\rangle$ direction, which has a local minima at $1/6\langle 1\bar{2}10\rangle$. Our calculated γ-surfaces are in reasonable agreement with the previous DFT calculations.[2,19]

Now, we study the effect of β-stabilizers elements (W, Mo, V, Ta, and Nb) on the stacking fault energies of α-Ti. Fig. 3 shows the results of GSFE curves for pure Ti and Ti-X alloys for the basal and prismatic slip systems with two different concentrations of alloying element at the fault plane. The two maxima for the basal fault refer to the unstable stacking fault (γ_{USF}) and the unstable twin fault (γ_{UT}), respectively, and the two minima refer to the stable stacking fault (γ_{SF}) and the stable twin fault (γ_{TE}). The predicted stacking fault energies for the basal slip of pure α-Ti using 48 and 80 atoms supercells are 302 mJ/m^2 and 298 mJ/m^2, respectively, which are converged to within 0.01% of each other. On the other hand, Ti prismatic stacking fault energies from 96 and 160 atoms supercells are 248 mJ/m^2 and 217 mJ/m^2, respectively. This larger difference relates to the number of atomic planes that was used in these two supercells. Therefore, to characterize the effect of the number of atomic planes on the prismatic stacking fault energy, different supercells with different number of atomic planes have been used for pure α-Ti to determine the

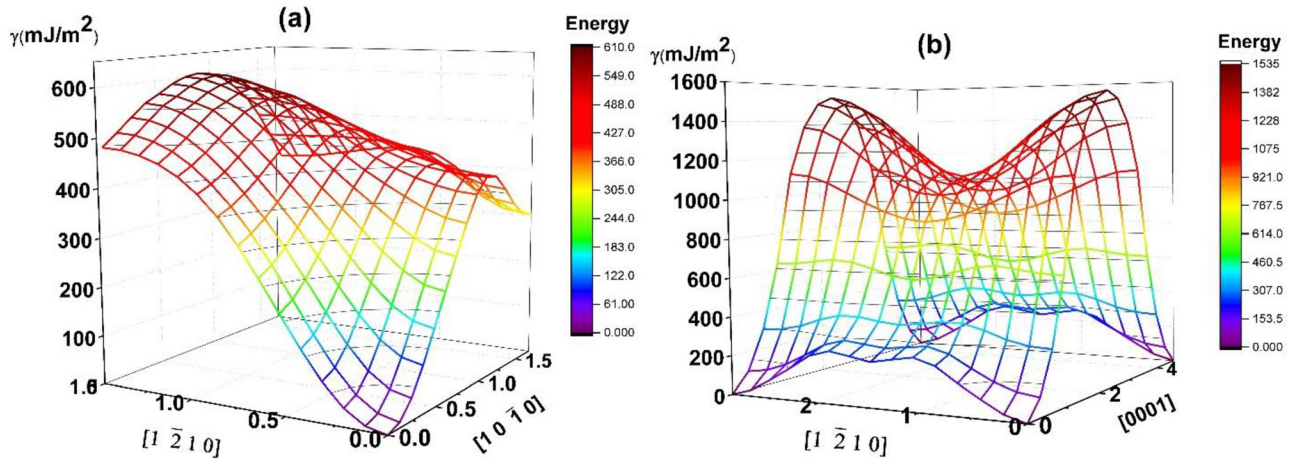

FIG. 2. γ-surface for basal (a) and prismatic (b) slips in pure α-Ti.

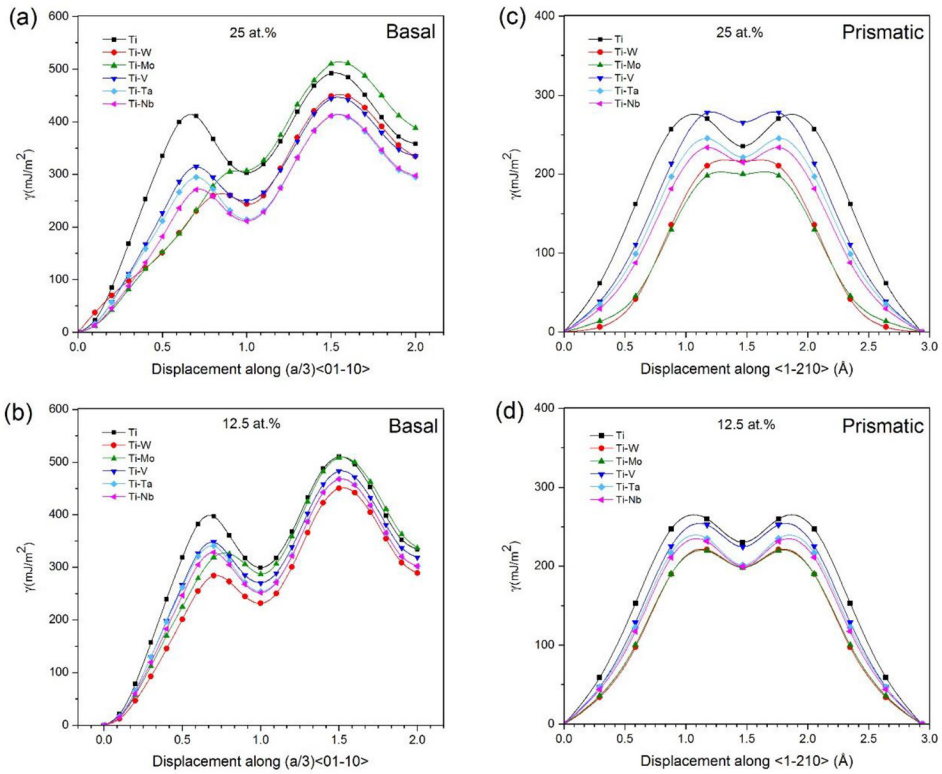

FIG. 3. (a) and (b) GSFE curves for basal slip. (c) and (d) GSFE prismatic slip for Ti and Ti-X alloys with two different compositions at the fault plane.

number of atomic planes that gives the most converged result. Fig. 4 presents the prismatic stacking fault energy of α-Ti as a function of inverse number of atomic planes. As can be seen, the values fluctuate with the number of atomic planes. However, the prismatic stacking fault energy starts to converge with number of atomic planes greater than 16 with a small but acceptable oscillation. A similar dependence of prismatic stacking fault energy for α-Ti with the number of atomic plane has been reported by Benoit *et al.*[2] In this work, the average value of the prismatic stacking fault energy has been considered for pure α-Ti which is 231 mJ/m^2, whereas supercells with atomic planes number greater than 16 have been considered for all other Ti-X systems. The range of basal stacking fault energy in literatures is 287 mJ/m^2 (Ref. 20) to 319 mJ/m^2 (Ref. 21), and the prismatic stacking fault energy ranges from 220 mJ/m^2 (Ref. 19) to 250 mJ/m^2.[2] Our calculated basal and prismatic stacking fault energy values of 302 mJ/m^2 and 231 mJ/m^2 agree with the literatures values. For the prismatic faults, the local minimum or the metastable point at b/2 indicates a possible dissociation into partial dislocation. To the best of our knowledge, no first principle or experimental data have been reported for the GSFE of α-Ti with β-stabilizers elements to compare our results with, and our values are predictions.

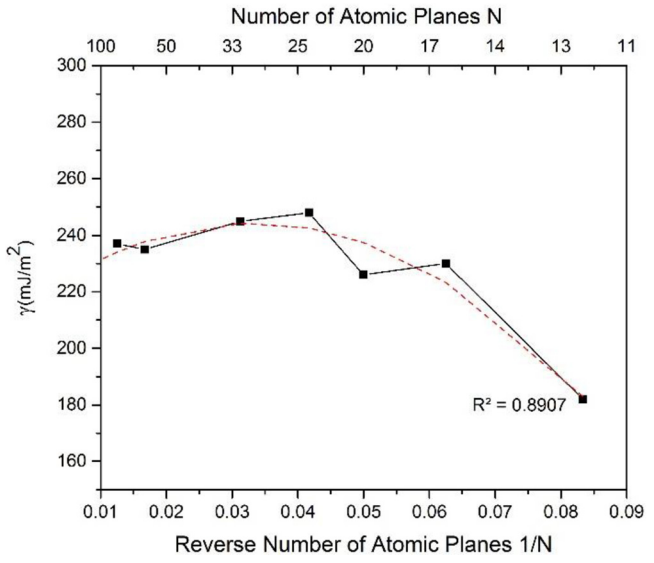

FIG. 4. Prismatic stacking fault energy of α-Ti as a function of inverse number of atomic planes 1/N.

Table I summarizes the calculated stacking fault energies for both 12.5 at. % and 25 at. % of alloying elements on

TABLE I. Calculated unstable stacking fault energy (γ_{USF}) and stable stacking fault energy (γ_{SF}) for the basal and prismatic planes and twin fault energy (γ_{TE}) for Ti and Ti-X alloys are shown for two different solute concentrations. The energy values are in (mJ/m^2).

Ti-X	X_{FP}%	γ_{USF}	γ_{SF}	γ_{UT}	γ_{TE}	$\gamma_{Prismatic}$	γ_{SF}/γ_{USF}	γ_{UT}/γ_{USF}
Ti		410.7	302.8	493	357.6	231	0.73	1.2
Ti-W	25	259.9	243.7	452	334	216	0.93	1.28
Ti-Mo	25	304	306.6	513.2	388	199.8	1	1.68
Ti-V	25	314.2	249.5	446.7	334.6	265.3	0.79	1.42
Ti-Ta	25	293	214	413	294.5	221.2	0.73	1.4
Ti-Nb	25	270	211.3	404.9	286.9	214.5	0.81	1.42
Ti-W	12.5	284	231.6	450.3	289	198.3	0.81	1.58
Ti-Mo	12.5	325.9	286.8	509	336.8	197.7	0.88	1.56
Ti-V	12.5	347.8	270	483.2	318.8	224	0.77	1.38
Ti-Ta	12.5	340.9	254.1	468	301.9	201	0.74	1.37
Ti-Nb	12.5	328.4	252	467.6	301.9	199	0.76	1.42

the fault plane. It should be noted that many random configurations of solute atoms are possible and all the concentrations considered in this study are the best compromise we could obtain between the number of atoms in the supercell and the number of atomic planes that avoid having the next nearest neighbors solute atoms at the fault plane.

For the basal slip in Fig. 3(a) with 25 at. % local concentration at the fault plane, which corresponds to 2.08 at. % global concentration using the 48 atoms supercell, it can be seen that all of the alloying elements decrease the stable (γ_{SF}) and unstable (γ_{USF}) stacking faults energies for Ti basal faults except Mo, which increases the stable stacking fault energy. Ta and Nb greatly reduce the stacking fault energy followed by W and V. Also, the alloying elements, with the exception of Mo, reduce the twin formation energy (γ_{TE}). It is remarkable to see that the Mo stacking fault energy curve maximum has been shifted to a higher value of a/3$\langle 01\bar{1}0\rangle$ and does not show a minimum compared with Ti and other Ti-X alloys. We will discuss this observation later.

For the prismatic faults in Fig. 3(c), with 25 at. % local concentration at the fault plane using 96 atoms supercell, all alloying elements decrease the stacking fault energies for Ti except V, which increases it. Also, W and Mo do not show a metastable point like the other elements considered here. It is theoretically and experimentally observed that Ti has a dominant prismatic slip system,[22,23] but this preference is altered by alloying. If we compare the stacking faults energies for basal and prismatic slip systems of 25 at. % alloys, we notice that Ta, Nb, and V increased the prismatic stacking faults energy above the basal stacking fault energies, so the basal slip in this case becomes more favorable than the primary prismatic slip. A similar effect was predicted when Al is added to Ti.[6,24]

Fig. 3(b) shows the basal GSFE curves for the 12.5 at. % solute concentration at the basal fault plane using 80 atoms supercell. We can see that the alloying elements reduce the stacking fault energies, but this reduction is less than in the 25 at. % concentration case, which is likely due to the decreasing interaction between solute atoms at the fault plane. This is evident in the behavior of Ti-Mo, where the unstable stacking fault energy γ_{USF} has been shifted smaller displacement along a/3$\langle 01\bar{1}0\rangle$ than the higher concentration case, Fig. 2(a). All elements reduce the stable (γ_{SF}) and unstable (γ_{USF}) stacking faults energies for the basal slip, but this reduction is not sufficient enough to make the basal slip more favorable than the prismatic slip for V, Ta, and Nb as was the case at higher concentration. Also, W shows the highest reduction in the stacking fault energy and twin fault energy at this concentration.

Fig. 3(d) shows the prismatic GSFE curves for 12.5 at. % solute at the fault plane. The stacking fault energy curves show the same trends as in systems with higher concentration of solutes. However, V decreases the stacking fault energy for Ti at this lower solute concentration. Table I shows that the prismatic stacking fault energies at this lower concentration are less than the basal stacking faults energies for the same concentration. Therefore, the prismatic slip in this case is the preferred slip system in Ti.

We now examine how solute affects deformation of α-Ti using the models of Tadmor and Bernstein,[25,26] and Rice.[27] We know that the reduction of the stacking fault energy enhances partial dislocation emission and increases the strength by restricting the dislocation slip if this reduction results in narrow spaced faults.[28] The stable stacking fault energy is inversely proportional to the distance between the two Shockley partials, which result from dissociation. An increase in separation distance between partials in turn causes a reduction in cross slip, and climb of dislocations. In addition, the mechanical properties of Ti can be modified by having more than one active slip system. Our results show that this can be achieved by having high concentration of V, Ta, and Nb alloying elements at the slip plane. The activation of the basal slip in addition to the prismatic slip will enhance the ductility and increase the strength when *β*-stabilizers solutes are added to α-Ti. The addition of these alloying elements decreases the force for dislocation splitting.

Tadmor and Bernstein[25,26] suggested the use of γ_{SF}/γ_{USF} and γ_{UT}/γ_{USF} ratios to predict the propensity for twinning in the face-centered cubic (fcc) lattice. The reduction of γ_{SF}/γ_{USF} ratio increases the emission of partial dislocation, and a lower γ_{UT}/γ_{USF} ratio means more twinning tendency. Based on this work and assuming a similar behavior for hcp lattice of fcc lattice, we calculated these two ratios in Table I. Based on this model, we see that these alloying elements do not improve the partial dislocation emission or the twinning propensity in spite of the decrease in the stacking fault energies for α-Ti.

Rice proposed a different criterion to predict the intrinsic ductility of a material using the ratio γ_S/γ_{USF},[27] where γ_S is the surface energy. If the surface energy is large when compared with the unstable stacking fault energy, the metal tends to deform by shear under an applied stress instead of forming surfaces via cracking. We will consider the surface energies and unstable stacking fault energies for the basal and prismatic slip systems. The values of γ_S/γ_{USF} ratios are shown in Fig. 5. It can be seen that for 12.5 at. % and 25 at. % Ti-Nb systems show the most ductile behavior for the prismatic and basal slip, respectively. Note that we excluded the Ti-W system from the ductility consideration because its γ_{USF} shows a shift towards a higher displacement of

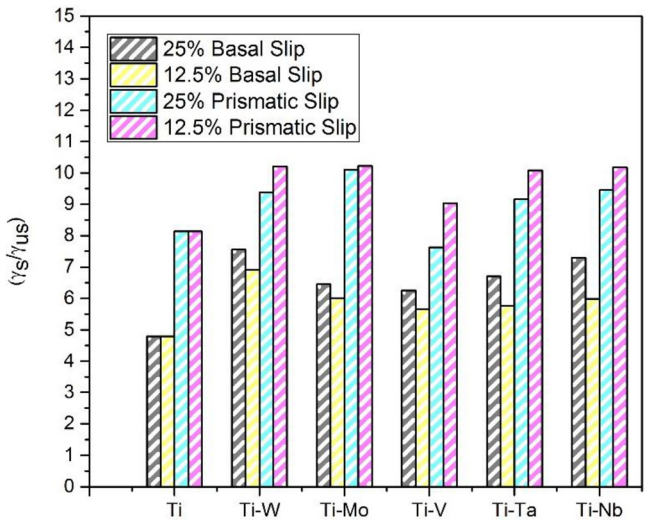

FIG. 5. The ratios of γ_S/γ_{USF} for Ti-X alloys with different concentrations of alloying elements in the basal and prismatic fault planes.

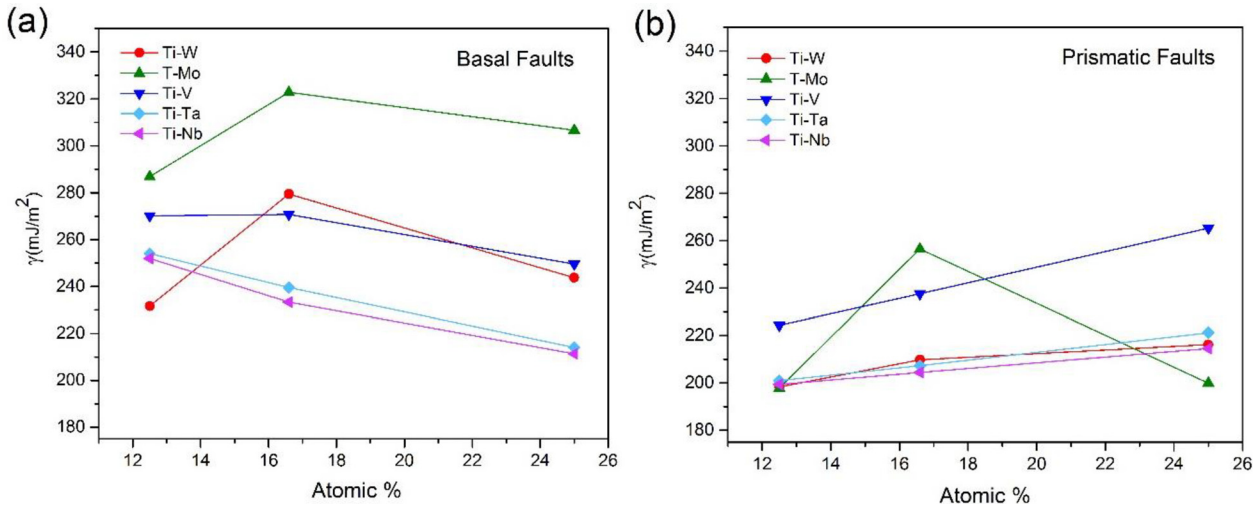

FIG. 6. Stable stacking fault energies γ_{SF} with different concentrations of alloying elements at the slip plane for basal slip (a) and prismatic slip (b).

$a/3\langle 01\bar{1}0\rangle$ in the GSFE curve, and this will be discussed further later. For the prismatic slip, the Ti-Mo system shows the most ductile behavior according to the Rice criterion for the 25 at. %. For the 12.5 at. % cases, the alloying elements affect the ductility similarly except V which shows the least ductile behavior at this concentration. However, this criterion may not clearly indicate the ductility behavior of solutes because it does not account for the different bond morphologies that may develop with different alloying elements. It is worth mentioning that using other criteria like the Legrand's ratio[29] may give a better picture on the effect of these alloying elements on the slip preference and ductility of Ti-X alloys, and this will be the subject of the future work.

To get a better trend of the effect of alloying elements on the stacking fault energy of Ti, the stable stacking fault energy γ_{SF} was also determined for 16.6 at. % solute at the fault plane, as shown in Fig. 6.

Fig. 6(a) shows that the basal stacking fault energy (γ_{SF}) decreases as the concentration of V, Ta, and Nb solutes increases, but this is not the case for W and Mo where the stacking fault energy increases for the 16.6 at. % concentration and decreases when the concentration reaches 25 at. %. This unusual behavior of W and Mo suggests the presence of different types of bonding between these two elements and Ti when their concentration changes at the basal slip plane.

Fig. 6(b) shows that the prismatic stacking fault energy (γ_P) increases with increasing concentration of all solutes with one exception of Mo: Mo drastically increased the stacking fault energy at 16.6 at. %. We further investigated the unusual effect of Mo on the stacking fault energy of Ti. Fig. 7 shows the variations of basal and prismatic stacking fault energies of Ti-Mo system with five different concentrations. Achieving these concentrations for the basal slip without having the next nearest neighbors of solute atoms at the fault plane required relatively huge supercells with many Mo atoms at the fault plane, and this has been done by constructing two supercells with 300 atoms and 360 atoms.

Ti-Mo systems show an increase in the stacking fault energy for the basal slip with increasing concentration, reach its maximum at 16.6 at. %, decrease afterwards, and fluctuate within 298 (mJ/m^2) and 307 (mJ/m^2) for 20 and 25 at. %, respectively. The only concentration that produces a significant decrease in Ti-Mo system's stacking fault energy for the basal slip is 12.5 at. %. For the prismatic slip system, the stacking fault energy increases with increasing concentration of Mo from 12.5 at. % to 16.6 at. %. It reaches a maximum at 16.6 at. % and gradually decreases after that with increasing Mo concentration. From the above, we can conclude that there is a turning point for Ti-Mo system where its stacking fault energy reaches a maximum for both basal and prismatic slip systems, and this point maxima occurs approximately at 16.6 at. % Mo.

The mechanical properties of materials relate to the atomic bonding. So, we now correlate the effect of concentration on the stacking fault energy with the nature of bonding between Ti and the solute atoms. The differential charge density ($\Delta\rho$) is used qualitatively to examine the bond structure of the materials.[30,31] Such an approach has been used previously to study Al and Mg.[32,33] An alloying element may

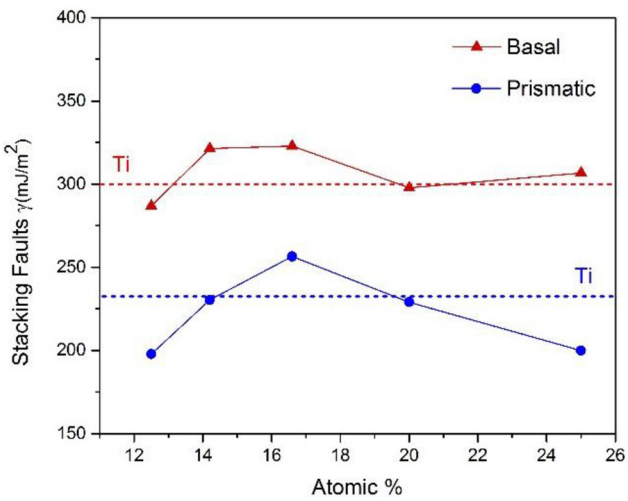

FIG. 7. Basal and prismatic stacking fault energies for Ti-Mo system with different concentrations at the slip plane. The horizontal dashed lines mark SF energy values in pure α-Ti.

modify the stacking fault energy by changing the charge density distribution, and higher stacking fault energy correlates with strong bonding, which depends on the density and shape of the electronic charge density.[4,34] We will examine the effects of β-stabilizer elements (W, Mo, V, Ta, and Nb) on the charge density difference of Ti to explain the stacking fault energy changes and the shape of the generalized stacking fault energy curves for Ti-X alloys. The differential charge density for Ti-X alloys was obtained by subtracting the non-interacting charge density, which is the charge density after one electronic step from the total charge density accruing after complete electronic relaxations.[35]

Fig. 8(a) shows a 3-D isosurface plot for differential charge density of Ti-12.5X systems at the stable stacking fault configuration. As seen from this figure, a higher density of electrons is seen around Mo and W, and lower density of electrons is around V, Ta, and Nb. Higher density of electrons is indicative of an enhancement of covalent character and therefore stronger bonds.

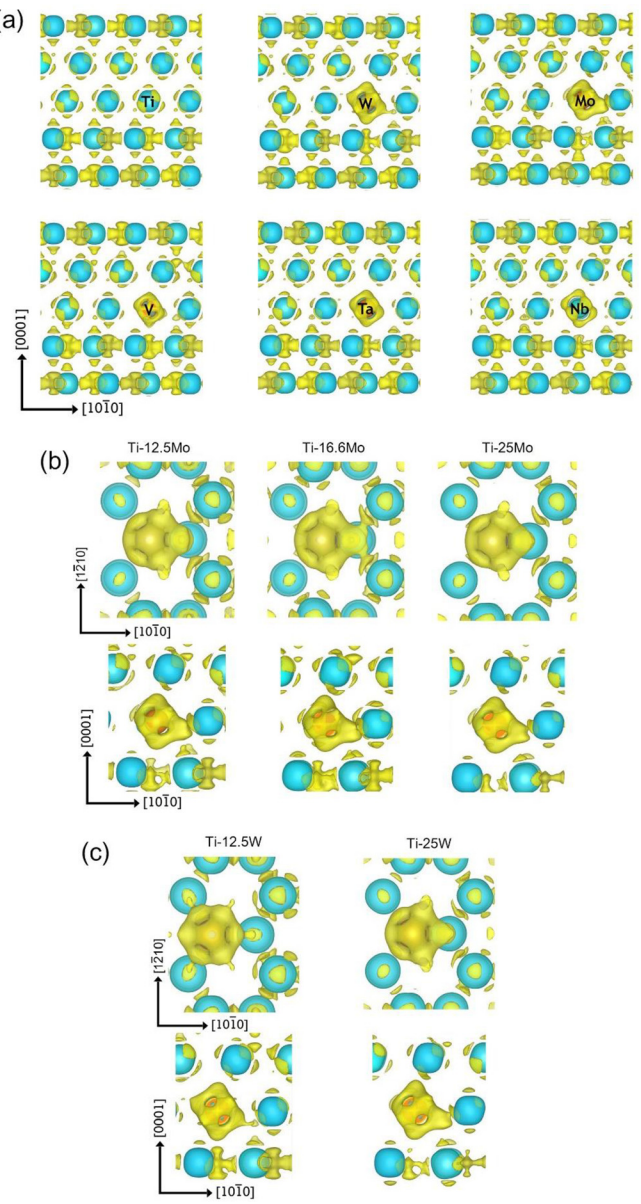

FIG. 8. (a) A 3D-isosurfcae plot of differential charge density ($\Delta\rho$) of Ti-X systems, X = W, Mo, V, Ta, and Nb. (b) Two views of Ti-Mo system are shown for three concentrations. (c) Two views of Ti-W system are shown for two concentrations. The yellow and cyan colors refer to charge accumulation and depletion, respectively, and an isosurface level of 0.0135 eV^{-3} has been used to visualize the charge density in all these plots.

In Figs. 3(a) and 3(b), we can see that the generalized stacking fault energy curves for Ti-Mo systems are displaced and do not match the behavior of other alloying elements, suggesting a presence of a different type of bonding between Ti and Mo. The non-uniform distribution of the charge density around Mo gives us the indication of bond directionality along $\langle 01\bar{1}0\rangle$ direction. The same behavior of Mo has been observed in β-Ti[36] where it was seen that the bond character varies with the concentration of Mo and ranges from ionic at high concentration to covalent and less covalent at lower concentrations. This is what we observe in Fig. 8(b) that a higher anisotropic charge distribution occurs around Mo at 16.6 at. % where Ti-Mo system shows the highest stacking fault energy. This correlates with a strong directional bonding between Ti and Mo at this concentration, while a lower anisotropic charge distribution around Mo can be observed at 12.5 at. % and 25 at. %. Fig. 8(c) illustrates the charge density difference in the Ti-W system at 12.5 at. % and 25 at. %. We notice the bond directionality for 25 at. % disappeared at 12.5 at. %, thereby explaining the displacement of stable and unstable stacking fault energies towards a higher shear deformation range along $\langle 01\bar{1}0\rangle$ and the normal shape of the stacking fault energy curve for Ti-25 at. % W and Ti-12.5 at. % W, respectively, as it has been observed in Figs. 1(a) and 1(b). The directional bonding gives the alloy an ability to accommodate a larger range of shear deformation range, which likely increases the ideal shear strength of the alloy.

IV. CONCLUSION

A systematic first principles study has been conducted to calculate the GSFE curves for basal I2 and prismatic slip systems of five α-Ti binary alloys and compared them with pure α-Ti. The five β-stabilizer solutes used include W, Mo, V, Ta, and Nb. Our results of the gamma surface revealed a preference for prismatic spreading along $\langle 1\bar{2}10\rangle$ slip over the basal slip along $\langle 01\bar{1}0\rangle$ in pure α-Ti. Using different compositions between 25 at. % and 12.5 at. % for each slip system at the fault plane, we observed that the basal slip becomes more favorable than the prismatic slip by alloying Ti with 25 at. % of V, Ta, and Nb. The highest reduction in basal and prismatic stacking fault energies occurs in Ti-Nb and Ti-Mo systems, respectively, with 25 at. % concentration of these alloying elements at the fault plane. 25 at. % V increases in the stacking fault energy for the prismatic slip. Tadmore and Bernstein model indicated that our alloying elements do not improve in the partial dislocation emission or the twinning propensity in spite of the decrease in the stacking fault energies for α-Ti. On the other hand, Rice criterion revealed that all solute elements likely improve ductility of α-Ti. This improvement in alloying Ti with 25 at. % of V, Ta, and Nb is due to the activation of both the basal and dominant prismatic slips. The stacking fault energy value for the Ti-Mo

system varies with the Mo concentration at the fault plane and reaches a maximum at 16.6 at. % for both the basal and prismatic slips, likely due to the variation of Ti-Mo bonding. The charge density difference ($\Delta\rho$) for the Ti-Mo system shows a high anisotropic charge distribution around Mo at 16.6 at. %, which corresponds to the highest stacking fault energy in the Ti-Mo system. We can attribute this to a strong directional bonding between Ti and Mo at this concentration. Therefore, the shift towards a higher shear deformation range along $\langle 01\bar{1}0\rangle$ in the GSFE curve for the Ti-Mo system is likely due to the non-uniform distribution of the charge density around Mo. Also, the anisotropic charge density difference in the Ti-W system indicates that the bond directionality that exists for Ti-25 at. % disappeared at a lower 12.5 at. % concentration. Hence, there is a need to formulate a physics-based empirical model that faithfully incorporates the changes in the character of directional bonding upon alloying. Finally, the results of this work can be used as a theoretical basis to enhance the current knowledge about Ti alloys and their plastic behavior at the atomic level in order to design a new α-Ti alloys, which have a better ductility and strength.

ACKNOWLEDGMENTS

This work was supported by the NSF DEMREF program (grant number 1435611). The computations were done on Talon2 and Stampede supercomputers at the University of North Texas and Texas Advanced Computing Center (TACC) at Austin. The authors also thank Dr. N. Gupta for his help.

[1]S. Sandlöbes, M. Friák, S. Zaefferer, A. Dick, S. Yi, D. Letzig, Z. Pei, L. F. Zhu, J. Neugebauer, and D. Raabe, "The relation between ductility and stacking fault energies in Mg and Mg-Y alloys," Acta Mater. **60**(6–7), 3011–3021 (2012).
[2]M. Benoit, N. Tarrat, and J. Morillo, "Density functional theory investigations of titanium γ -surfaces and stacking faults," Modell. Simul. Mater. Sci. Eng. **21**(1), 15009 (2013).
[3]V. Vítek, "Intrinsic stacking faults in body-centred cubic crystals," Philos. Mag. **18**(154), 773–786 (1968).
[4]S. L. Shang, W. Y. Wang, B. C. Zhou, Y. Wang, K. A. Darling, L. J. Kecskes, S. N. Mathaudhu, and Z. K. Liu, "Generalized stacking fault energy, ideal strength and twinnability of dilute Mg-based alloys: A first-principles study of shear deformation," Acta Mater. **67**, 168–180 (2014).
[5]C. Tian, G. Han, C. Cui, and X. Sun, "Effects of stacking fault energy on the creep behaviors of Ni-base superalloy," Mater. Des. **64**, 316–323 (2014).
[6]Z. Guo, A. P. Miodownik, N. Saunders, and J. P. Schillé, "Influence of stacking-fault energy on high temperature creep of alpha titanium alloys," Scr. Mater. **54**(12), 2175–2178 (2006).
[7]P. L. Sun, Y. H. Zhao, J. C. Cooley, M. E. Kassner, Z. Horita, T. G. Langdon, E. J. Lavernia, and Y. T. Zhu, "Effect of stacking fault energy on strength and ductility of nanostructured alloys: An evaluation with minimum solution hardening," Mater. Sci. Eng., A **525**(1–2), 83–86 (2009).
[8]B. J. Q. Ren and M. S. Duesbery, "Peierls-Nabarro model of dislocations in silicon with generalized stacking-fault restoring forces," Phys. Rev. B **50**(9), 5890–5898 (1994).
[9]P. Kwasniak, M. Muzyk, H. Garbacz, and K. J. Kurzydlowski, "Influence of C, H, N, and O interstitial atoms on deformation mechanism in titanium - First principles calculations of generalized stacking fault energy," Mater. Lett. **94**, 92–94 (2013).
[10]M. Ghazisaeidi and D. R. Trinkle, "Interaction of oxygen interstitials with lattice faults in Ti," Acta Mater. **76**, 82–86 (2014).
[11]M. A. Bhatia, X. Zhang, M. Azarnoush, G. Lu, and K. N. Solanki, "Effects of oxygen on prismatic faults in α-Ti: A combined quantum mechanics/molecular mechanics study," Scr. Mater. **98**, 32–35 (2015).
[12]V. Vitek and M. Igarashi, "Core structure of $\frac{1}{3}\langle 1120\rangle$ screw dislocations on basal and prismatic planes in h.c.p. metals: An atomistic study," Philos. Mag. **63**(5), 1059–1075 (1991).
[13]G. Kresse and J. Hafner, "Molecular dynamics for liquid metals," Phys. Rev. B **47**(1), 558–561 (1993).
[14]G. Kresse, "Efficient iterative schemes for *ab initio* total-energy calculations using a plane-wave basis set," Phys. Rev. B **54**(16), 11169–11186 (1996).
[15]P. E. Blöchl, "Projector augmented-wave method," Phys. Rev. B **50**(24), 17953–17979 (1994).
[16]J. P. Perdew, K. Burke, and M. Ernzerhof, "Generalized gradient approximation made simple," Phys. Rev. Lett. **77**(18), 3865–3868 (1996).
[17]T. Uesugi, S. Miyamae, and K. Higashi, "Enthalpies of solution in Ti-X (X = Mo, Nb, V and W) alloys from first-principles calculations," Mater. Trans. **54**(4), 484–492 (2013).
[18]D. Raabe, B. Sander, M. Friák, D. Ma, and J. Neugebauer, "Theory-guided bottom-up design of β-titanium alloys as biomaterials based on first principles calculations: Theory and experiments," Acta Mater. **55**(13), 4475–4487 (2007).
[19]M. Ghazisaeidi and D. R. Trinkle, "Core structure of a screw dislocation in Ti from density functional theory and classical potentials," Acta Mater. **60**(3), 1287–1292 (2012).
[20]X. Wu, R. Wang, and S. Wang, "Generalized-stacking-fault energy and surface properties for HCP metals: A first-principles study," Appl. Surf. Sci. **256**(11), 3409–3412 (2010).
[21]A. Poty, J. M. Raulot, H. Xu, J. Bai, C. Schuman, J. S. Lecomte, M. J. Philippe, and C. Esling, "Classification of the critical resolved shear stress in the hexagonal-close-packed materials by atomic simulation: Application to -zirconium and -titanium," J. Appl. Phys. **110**(1), 0–15 (2011).
[22]N. Tarrat, M. Benoit, D. Caillard, L. Ventelon, N. Combe, and J. Morillo, "Screw dislocation in hcp Ti : DFT dislocation excess energies and metastable core structures," Modell. Simul. Mater. Sci. Eng. **22**(5), 55016 (2014).
[23]M. H. Yoo, J. R. Morris, K. M. Ho, and S. R. Agnew, "Nonbasal deformation modes of HCP metals and alloys: Role of dislocation source and mobility," Metall. Mater. Trans. A **33**(13), 813–822 (2002).
[24]J. C. Williams, J. C. Williams, R. G. Baggerly, R. G. Baggerly, N. E. Paton, and N. E. Paton, "Deformation behavior of HCPTi-Al alloy single crystals," Metall. Mater. Trans. A **33**(3), 837–850 (2002).
[25]E. B. Tadmor and N. Bernstein, "A first-principles measure for the twinnability of FCC metals," J. Mech. Phys. Solids **52**(11), 2507–2519 (2004).
[26]N. Bernstein and E. Tadmor, "Tight-binding calculations of stacking energies and twinnability in fcc metals," Phys. Rev. B **69**(9), 1–10 (2004).
[27]J. R. Rice, "Dislocation nucleation from a crack tip: an analysis based on the peierls concept," J. Mech. Phys. Solids **40**(2), 239–271 (1992).
[28]W. W. Jian, G. M. Cheng, W. Z. Xu, H. Yuan, M. H. Tsai, Q. D. Wang, C. C. Koch, Y. T. Zhu, and S. N. Mathaudhu, "Ultrastrong Mg alloy via nano-spaced stacking faults," Mater. Res. Lett. **1**(2), 61–66 (2013).
[29]P. B. Legrand, "Structure du coeur des dislocations vis $1/3\langle 1120\rangle$ dans le titane," Philos. Mag. A **52**(1), 83–97 (1985).
[30]P. N. H. Nakashima, A. E. Smith, J. Etheridge, and B. C. Muddle, "The bonding electron density in aluminum," Science **331**(6024), 1583–1586 (2011).
[31]P. A. Midgley, "Electronic bonding revealed by electron diffraction," Science **331**(6024), 1528–1529 (2011).
[32]S. Ogata, J. Li, and S. Yip, "Ideal pure shear strength of aluminum and copper," Science **298**(5594), 807–811 (2002).
[33]W. Y. Wang, S. L. Shang, Y. Wang, K. A. Darling, S. N. Mathaudhu, X. D. Hui, and Z. K. Liu, "Electron localization morphology of the stacking faults in Mg: A first-principles study," Chem. Phys. Lett. **551**, 121–125 (2012).
[34]Y. Qi and R. Mishra, "*Ab initio* study of the effect of solute atoms on the stacking fault energy in aluminum," Phys. Rev. B **75**(22), 1–5 (2007).
[35]S. Ganeshan, L. G. Hector, and Z. K. Liu, "First-principles calculations of impurity diffusion coefficients in dilute Mg alloys using the 8-frequency model," Acta Mater. **59**(8), 3214–3228 (2011).
[36]M. Lai, X. Xue, Z. Zhou, B. Tang, J. Li, and L. Zhou, "First-principles prediction of ductility in β-type Ti-Mo binary alloys," J. Shanghai Jiaotong Univ. **16**(2), 227–230 (2011).